EPJ E
Soft Matter and Biological Physics
EPJ.org
your physics journal

Eur. Phys. J. E (2013) **36**: 77 DOI 10.1140/epje/i2013-13077-0

Influence of charge density on bilayer bending rigidity in lipid vesicles: A combined dynamic light scattering and neutron spin-echo study

B. Brüning, R. Stehle, P. Falus and B. Farago

edp sciences Società Italiana di Fisica Springer

Eur. Phys. J. E (2013) **36**: 77
DOI 10.1140/epje/i2013-13077-0

THE EUROPEAN PHYSICAL JOURNAL E

Regular Article

Influence of charge density on bilayer bending rigidity in lipid vesicles: A combined dynamic light scattering and neutron spin-echo study*

B. Brüning[1,a], R. Stehle[1], P. Falus[2], and B. Farago[2]

[1] Helmholtz Zentrum Berlin, Hahn-Meitner Platz 1, 14109 Berlin, Germany
[2] Institut Laue-Langevin, B.P. 156, 38042 Grenoble, France

Received 2 August 2012 and Received in final form 18 December 2012
Published online: 17 July 2013 –

Abstract. We report a combined dynamic light scattering and neutron spin-echo study on vesicles composed of the uncharged stabilizing lipid 1,2-dimyristoyl-sn-glycero-3-phosphatidylcholine (DMPC) and the cationic lipid 1,2-dioleoyl-3-trimethylammonium-propane (DOTAP). Mechanical properties of a model membrane and thus the corresponding bilayer undulation dynamics can be specifically tuned by changing its composition through lipid headgroup or acyl chain properties. We compare the undulation dynamics in lipid vesicles composed of DMPC/DOTAP to vesicles composed of a mixture of the uncharged helper lipid DMPC with the also uncharged reference lipid 1,2-dioleoyl-sn-glycero-3-phosphocholine (DOPC). We have performed dynamic light scattering on the lipid mixtures to investigate changes in lipid vesicle size and the corresponding center-of-mass diffusion. We study lipid translational diffusion in the membrane plane and local bilayer undulations using neutron spin-echo spectroscopy, on two distinct time scales, namely around 25 ns and around 150 ns. Finally, we calculate the respective bilayer bending rigidities κ for both types of lipid vesicles. We find that on the local length scale inserting lipid headgroup charge into the membrane influences the bilayer undulation dynamics and bilayer bending rigidity κ less than inserting lipid acyl chain unsaturation: We observe a bilayer softening with increasing inhomogenity of the lipid mixture, which could be caused by a hydrophobic mismatch between the acyl chains of the respective lipid components, causing a lateral phase segregation (domain formation) in the membrane plane.

1 Introduction

Phospholipids and liposomes play a prominent role as model systems to understand basic properties of their far more complex biological counterparts, since in mammal organisms vesicles often serve as natural carriers (*e.g.* red blood cells, synaptic vesicles). The natural occurrence of such vesicular carriers is often mimicked in colloid and interface science. In particular, liposomes composed of cationic lipids and varying helper molecules have been found to be effective vehicles for cellular delivery of drug formulations [1–3], as well as RNA and DNA [4–6]. In this context, a detailed understanding of changes in bilayer properties induced by the charged lipid headgroups is crucial in order to aimfully exploit their potential as targeted carriers. Lipid mixtures containing cationic lipid and a helper lipid have been studied in great detail with respect to vesicle size, aggregation behaviour and stability of the complexes [7–9], thermodynamic properties and phase behaviour [10], as well as their suitability as colloidal carriers for specific purposes. For example, liposomes designated for gene transfection require intrinsic instability, whereas vesicles for drug delivery often contain more stabilizing lipids. Changes in vesicle stability can be induced *e.g.* through variation of the lipid head group composition or the degree of acyl chain unsaturation [11,12].

Compared to morphological and thermodynamic aspects, the local lipid bilayer undulation dynamics of fluid cationic liposomes has, to our knowledge, not been studied so far, even though functional properties of the membrane interface may depend equally on vesicle structure and dynamics. For uncharged lipid vesicles and model membranes oriented on a substrate, previous studies have shown the occurrence of dynamic processes over a broad range of length and time scales and by a variety of experimental techniques including neutron spectroscopy and molecular modelling [13–19]. In this context, several authors have mentioned that the respectively observed processes are somewhat hierarchically interlinked over several orders of length and time scales [19–24]. Neutron spin-

* Contribution to the Topical Issue "Neutron Biological Physics", edited by Giovanna Fragneto and Frank Gabel.

[a] e-mail: beate-annette.bruening@helmholtz-berlin.de

echo spectroscopy is well suited to probe dynamical processes well within the ns range, *i.e.* to perform quasielastic scattering experiments on the length scale of local interface undulations.

Binary phospholipid and lipid mixtures show a temperature- and composition-specific phase behavior, that includes the formation of large-scale mesoscopic domains, which exhibit lateral structure fluctuations in the membrane plane, between different coexisting phases [25, 26]. These characteristic fluctuations in the membrane plane have been studied in great detail in the past, and are assumed to have decisive influence on the mechanical properties of the lipid bilayer [26, 27]. Several experimental studies on microemulsions have addressed the influence of ionic surfactants on film undulations [28–30]. Recent studies on bilayer undulations in lipid vesicles have included those on lipids with acyl chain unsaturation [31], composite lipid membranes with cholesterol [19], the influence of changes in *p*H in pure zwitterionic phospholipid vesicles, as well as on the insertion of ibuprofen [32], or of pore-forming peptides [33]. Here, we extend this work towards alternative two-component model systems to shed light on the undulation dynamics in lipid mixtures containing charges, which are suitable as gene transfer or drug delivery agents. Moreover, we extend the dynamic range compared to previous neutron spin-echo experiments on lipid vesicles, such that a full polarization decay is obtained. Therefore, we can separate more precisely the influence of further contributions to the bilayer undulation dynamics, such as underlying vesicle center-of-mass diffusion. Next, we introduce the theoretical approach used to describe shape fluctuations as bending modes of an elastic membrane. This manner of treating the undulation dynamics in fluid phospholipid vesicles was already applied successfully in previous works, *e.g.* [19].

The paper is organized as follows: After this general introduction, a brief introduction is given to the theoretical description of film undulations in sect. 2, then sample preparation and experimental methods are presented in sect. 3, followed by dynamic light scattering results in sect. 4.1. Section 4.2 shows the central results on the lipid bilayer undulation and diffusive vesicle dynamics obtained by neutron spin-echo spectroscopy, before the paper closes in sect. 5 with conclusions and an outlook.

2 Theory

Curvature undulation dynamics of elastic membranes are commonly described by the well-known Helfrich Hamiltonian [34]. Based on this continuum mechanical approach, Milner and Safran further describe the fluctuation dynamics of microemulsion droplets and vesicles [35]. In their theory, the normal bending modes of the flexible interface are coupled to the viscous friction exerted by the suspending medium according to a single exponential decay $\exp(-\Gamma_{MS}t)$ with a relaxation rate $\Gamma_{MS} = \frac{\kappa}{4\eta}q^3$, where η is the effective viscosity of the solvent medium and κ the bilayer bending rigidity. In this manner, faster relaxations are assigned to stiffer membranes. However, while suited to describe data obtained from soft interfaces where the obtained bilayer bending rigidities lie on the order of k_BT, such as in microemulsion droplets and sponge phases, the expression fails to accurately account for the dynamics of model phospholipid membranes with expected bending rigidities on the order of several k_BT. In a phenomenological approach, Zilman and Granek introduce a model to describe curvature shape fluctuations of freely suspended phospholipid bilayers [36, 37]. Their model takes into account a coupling of the bending modes and local diffusion processes: in a rigid membrane with a bilayer bending rigidity of ($\kappa \gg k_BT$), less free volume can be explored by single molecules; this means that a relaxation rate for a coupled process of undulation and local curvature will increase, whereas the average amplitude of the modes will decrease. The anomalous subdiffusive relaxation of the bending motions is described by a stretched exponential decay (eq. (1))

$$S(q,t) \propto \exp(-\Gamma_u(q)\cdot t)^{\beta=0.66},$$

with

$$\Gamma_u(q) = 0.025\gamma_q \left(\frac{k_BT}{\kappa}\right)^{1/2} \cdot \left(\frac{k_BT}{\eta(T)}\right) q^3. \qquad (1)$$

Within the relaxation rate $\Gamma_u(q)$, $\eta(T)$ denotes the temperature-dependent solvent viscosity. Further, γ_q is a weak monotonous function of the bending rigidity κ according to $\gamma_q = 1 - \frac{3}{4\pi}(\frac{k_BT}{\kappa}) \cdot \ln(qh)$, where h is the membrane thickness with $q \cdot h \approx 1$. For lipid model membranes, where κ lies on the order of several k_BT, γ_q can be approximated to unity. In the following, we will discuss our data on the basis of the introduced model, augmented by the occurrence of underlying vesicle center-of-mass diffusion (eq. (2)).

$$S(q,t)/S(q,0) = A \cdot \exp(-\Gamma_d t) \cdot \exp(-\Gamma_u t)^{\beta}. \qquad (2)$$

Here, A is a normalization parameter close to one, the center-of-mass diffusion relaxation rate $\Gamma_d = D \cdot q^2$ is fixed using the diffusion constant D obtained by dynamic light scattering, the relaxation rate of bilayer undulations Γ_u is a free parameter, and the stretched exponential is held to $\beta = 0.66$, following the Zilman-Granek approach. Note that the product of the two dynamic contributions in (q,t)-space corresponds to the mathematical convolution of a Lorentzian and a Lorentzian-like function in the (q,ω)-space commonly viewed in quasielastic neutron scattering experiments performed with other techniques. Thus, our description with the two contributions seems to be more rigorous than to treat the data using a mere sum of the vesicle center-of-mass and bilayer undulation contributions as described *e.g.* in [19]. However, comparing the outcome to the results obtained on the basis of the previous description of the normalized intermediate scattering function $S(q,t)/S(q)$, no significant differences are obtained within experimental accuracy. This will be discussed in more detail later.

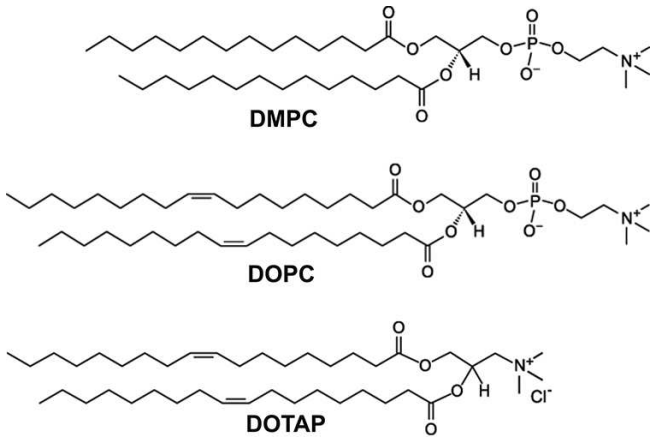

Fig. 1. Lipid molecules used in this study. From top: DMPC, DOPC and DOTAP (from: `http://avantilipids.com`).

3 Materials and methods

Sample preparation: The lipids (DMPC, DOPC, DOTAP) were purchased from Avanti (Alabaster, AL) (fig. 1) and dissolved in chloroform/TFE (1:1) in the desired molar proportions to achieve a homogenous mixture of the components. The solvent was evaporated slightly above room temperature in a vacuum oven and the dry lipids were hydrated with a concentration of 10 mg/ml in deuterated water (D_2O) obtained from Aldrich (Steinheim, Switzerland). To avoid possible differences between dynamic light scattering (DLS) and neutron spin-echo (NSE) experiments, D_2O was in all cases used as the aqueous solvent. Samples were then heated from room temperature up to 30 °C, ultrasonicated in a bath and cooled down to room temperature again several times subsequently. In order to obtain unilamellar vesicles (ULVs), the suspension consisting of multilamellar vesicles (MLVs) was passed ten times through a polycarbonate filter with 500 Å pore diameter using the LiposoFast Basic Extruder (Avestin, Canada).

For the neutron experiments, the extruded phospholipid suspensions were poured into (35 mm by 35 mm) quartz cells (1 mm thick, Hellma, Müllheim, Germany). These were then inserted into a thermostated sample holders, designated for use on the instrument.

Dynamic Light Scattering (DLS): For the dynamic light scattering (DLS) measurements, an ALV-4000 goniometer with a 35 mW He-Ne laser operating at a wavelength of 632.8 nm was used with an ALV/High QE APD detector and an ALV-6010/ 160 external multiple tau digital correlator unit. Angle-dependent measurements were taken between 20° and 150° in steps of 10°. Diffusion constants D derived from CONTIN and cumulant analysis up to the third order were compared. The differences between these approaches did not exceed the experimental error between independent measurements. From the ratio of the first- and second-order relaxation rates, a polydispersity index around 0.15 was obtained for all extruded vesicles. The diffusion coefficient D can be related to the hydrodynamic vesicle radius according to the Stokes-Einstein equation

$$R_H = \frac{k_B T}{6\pi \cdot \eta(T) \cdot D}\,. \tag{3}$$

Here, D denotes the mean diffusion coefficient, k_B the Boltzmann constant, T the absolute temperature and $\eta(T)$ the temperature-dependent solvent viscosity (for D_2O at 30 °C, $\eta(T) = 1.028 \cdot 10^{-3}$ Pa s). The lipid vesicles were prepared in varying compositions and investigated by DLS immediately after extrusion, as well as one week afterwards. For stable vesicles the hydrodynamic radius R_H remained the same within $\Delta R_H = \pm 2$ nm, which lies with the experimental errors. After extrusion through the polycarbonate membrane with a pore size of 50 nm, all vesicles had radii between 45 and 55 nm. However, at intermediate concentrations of the cationic lipid DOTAP (between 20 and 40 mol%), the vesicles quickly increased size to radii up to 70 and 80 nm. This was visible in the DLS measurements within one hour after the extrusion process, thus these concentrations were excluded from the spin-echo experiment.

Neutron Spin-Echo (NSE): The long-wavelength local bilayer undulation dynamics were investigated using the cold neutron spin-echo spectrometer IN15 at the Institut Laue Langevin (ILL in Grenoble, France). The instrument provides the longest wavelengths and Fourier times currently available on NSE spectrometers throughout the world. Due to its fine angular resolution in the small-angle regime (low q-values), the instrument is well suited to probe the mesoscopic lengths scales often encountered in colloidal systems. The method of neutron spin-echo spectroscopy (NSE) was first introduced by F. Mezei [38]. The result of a measurement consists of a momentum transfer and time-resolved intermediate structure factor $S(q,t)$. Contrary to the correlation functions $g(t)$ measured by dynamic light scattering, the q-range probed lies on the order of the inverse length scales of local bilayer interface undulations. This allows for a data interpretation on the basis of models predicting a specific q-dependence of the measured relaxation rates $\Gamma(q)$, such as *e.g.* the well-known approach of Zilman and Granek (eq. (1)). In the experiment, the momentum transfer is obtained from the scattering angle 2θ between the incoming and final beam, according to $q = \frac{4\pi}{\lambda} \cdot \sin\theta$. The method is described in more detail in [38].

The IN15 instrument is situated at a cold polarizing neutron guide. A velocity selector produces incident neutron wavelengths between 6 and 25 Å with a wavelength distribution of 10% (at the time the presented data was measured). At a distance of 4.6 m from the sample, the ^{3}He/CF4 multidetector is located, which covers $32 \cdot 32$ pixels of 1 cm^2 each for scattering angles between $2° \leq 2\theta \leq 22°$.

Primary data corrections include correction of the data with respect to instrumental resolution and solvent background. The instrumental resolution is determined by measuring graphoil as a purely coherent elastic scatterer.

The correction is performed by division of sample and resolution signal. The scattering of the D_2O solvent is mainly coherent and at the measured time scales well outside of the experimental window, resulting in a constant contribution which can be subtracted from the data.

4 Results and discussion

4.1 Dynamic light scattering (DLS)

For dynamic light scattering on vesicles with varying compositions, two main objectives were followed: The vesicle center-of-mass diffusion was quantified as an underlying contribution in the spin-echo data. Also, the corresponding temperature- and concentration-dependent phase behaviour and vesicle stability were monitored. This was considered necessary, as extruded phospholipid vesicles are non-equilibrium structures, due to the external force exerted on them during the process.

The relaxation rates Γ_d obtained from angle-dependent measurements are shown *vs.* q^2 for several lipid mixtures (fig. 2(a)). Linear fits (solid lines) match and exhibit a purely Fickian behaviour typical of center-of-mass diffusion. The slope of these curves corresponds to the mass diffusion constant D, from which the corresponding hydrodynamic radii R_H was derived (eq. (3)). Further, for all investigated lipid mixtures, temperature ramps from 10 °C to 60 °C were taken in steps of 5 °C in both directions, respectively (up and down). Measurements were performed at a constant scattering angle. For pure DMPC, a decrease in the hydrodynamic radius R_H is observed at the main phase transition near $T_m = 23.6$ °C. For composite lipid vesicles, the main transition occurs over a broader temperature range and at lower T_m (fig. 2(b)). In terms of the obtained phase transitions, we have compared our data to published phase diagrams [10, 39]. For vesicle compositions that were observed to remain stable for at least a week, neutron spin-echo data were taken at 30 °C. Here, the hydrodynamic radii R_H lay around 50 nm. Moreover, at a single lipid ratio, the vesicles exhibit stabilty within $\Delta R_H = \pm 2$ nm, while ramping up and down over the whole range of temperatures between 10 °C and 60 °C. In order to estimate possible inter-vesicle structure factor influences, exemplary samples were diluted down to 1 mg/ml concentration in D_2O solvent and remeasured. From the difference in the hydrodynamic radii R_H, we estimate structure factor influences of up to ten percent within the momentum transfer q-range covered by dynamic light scattering. Note that the inverse length scales q covered by dynamic light scattering and neutron spin-echo spectroscopy differ by three orders of magnitude. The influence of a structure factor is strongest in the regime of the small momentum transfers q covered by dynamic light scattering. We can therefore safely neglect its contribution at the large q covered by neutron spectroscopy. For the spin-echo experiment, we used mixtures of DMPC/DOTAP and DMPC/DOPC with unsaturated lipid ratios of 5 mol%, 10 mol% and 50 mol% at 10 mg/ml.

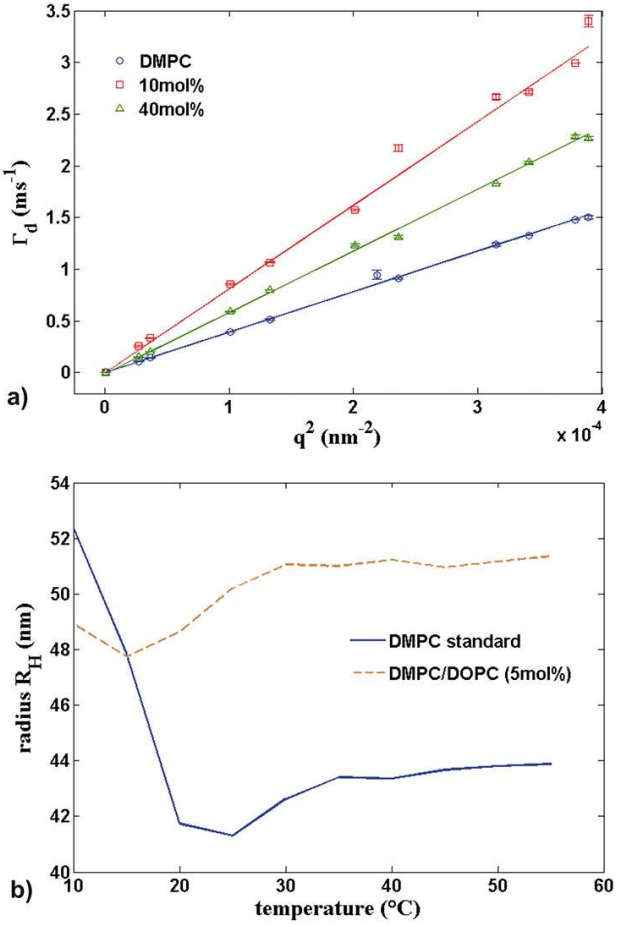

Fig. 2. (a) Relaxation rate Γ_d *vs.* momentum transfer q^2 for DMPC/DOTAP mixtures (30 °C). Solid lines represent linear fits, which yield the vesicle center-of-mass diffusion constant D; (b) hydrodynamic radius R_H *vs.* temperature T: For DMPC, a minimum in R_H is visible near the main phase transition at $T_m = 23.6$ °C. For composite vesicles, the transition occurs in a broader temperature range and at a lower T_m.

4.2 Neutron spin-echo (NSE)

The local lipid bilayer undulation dynamics was investigated by neutron spin-echo spectroscopy using two distinct wavelengths of $\lambda = 10$ Å and 18 Å. Therefore, we highlight varying dynamic regimes, taking advantage of an extended q-range at shorter wavelengths (the Fourier time range relates proportionally to the cubed incident wavelength). We first discuss overall dynamics observed at the shorter wavelength, thereby motivating our choice of a complementary (q, t)-regime to further separate different contributions. Together with the presented dynamic light scattering results, we use our findings for an interpretation of the data at the longer wavelength, where the two types of dynamical processes can be more quantitatively separated.

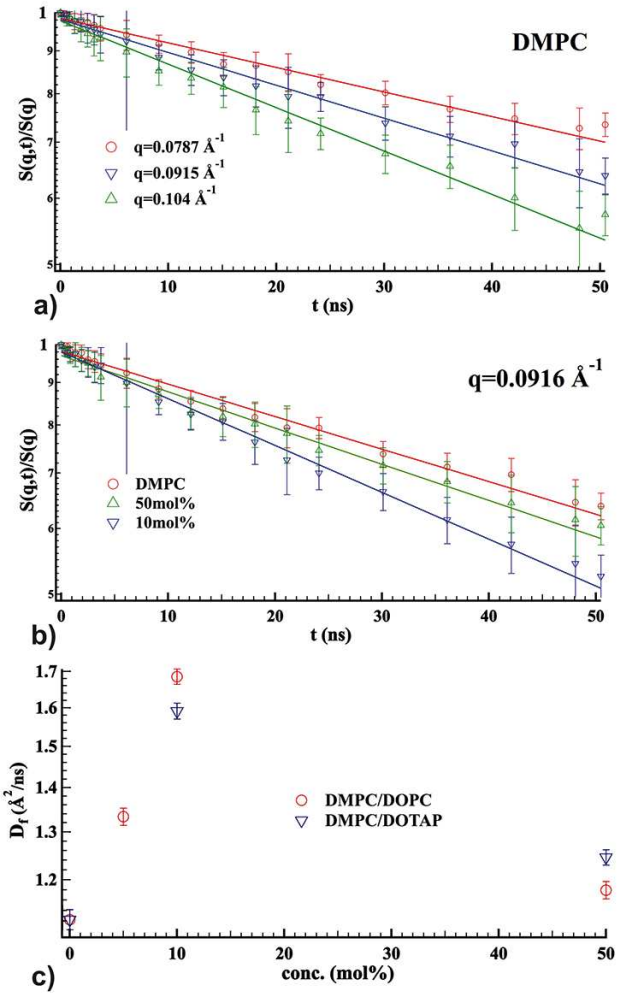

Fig. 3. Single-exponential fits of $S(q,t)/S(q)$ at $\lambda = 10\,\text{Å}$ (solid lines): (a) DMPC standard; (b) concentration dependence for DMPC/DOTAP lipid mixtures in varying molar ratios; and diffusion constant D_f from fits for DMPC/DOTAP lipid mixtures and the reference mixture DMPC/DOPC in varying molar ratios.

4.2.1 Short-wavelength dynamics: Lipid molecule translation

As a first step towards a more advanced data treatment, merely simple Fickian diffusion mechanisms were assumed at a wavelength of $\lambda = 10\,\text{Å}$, using single-exponential fits $S(q,t) \propto \exp(-\Gamma_f t)$, with $\Gamma_f = D_f \cdot q^2$. The data is shown in fig. 3(a) for the pure DMPC standard at varying momentum transfers q, then in (b) for DMPC/DOTAP with varying lipid ratios at a given q. In the following, concentrations of the lipid mixtures shall be denoted in mol% of the unsaturated lipid (DOPC or DOTAP, respectively). Solid lines in the figure indicate fits to the data. Single-exponential fits describe the data well within this particular dynamic range. With rising q the relaxation rate increases, resulting in a faster decay (a). In the same momentum tranfer range, the pure DMPC standard exhibits the weakest decay of all model liposomes, whereas the strongest decay is found for DMPC/DOTAP (10 mol%) (b). The diffusion constants D_f resulting from the described single-exponential fits, are then shown in (c) for the cationic DMPC/DOTAP liposomes at varying molar ratios of the unsaturated lipid, as well as for the corresponding uncharged DMPC/DOPC reference liposomes. For each liposome composition, the diffusion constant D_f was derived from linear fits of the relaxation rate $\Gamma_f(q^2)$ at five points in the q-range shown in (a). Within error bars, the obtained exponential decay Γ_f exhibits a maximum of equal magnitude at 10 mol% for both types of lipid mixtures. Whether this increase in the general dynamics could potentially be linked to a rise in the vehicular properties of a loaded vesicle, remains to be discussed.

Regarding the origin of the described mode, several possibilities exist: In their seminal theoretical works, Evans and Yeung, as well as Seifert and Langer have already predicted modes, which relate bending and local density changes between the two monolayers and taken into account resulting intermonolayer friction [40, 41]. The modes described follow quadratic dispersion relations $\Gamma(q^2)$, and have been discussed in recent experimental works by Arriaga *et al.* also using long-wavelength neutron spin-echo [23]. On the other hand, for DMPC at 30 °C, the diffusion constant of $D_f = 1.12\,\text{Å}^2/\text{ns}$ agrees with the ones found for lipid in-plane translational diffusion in previous experimental studies by Pfeiffer *et al.* [42], and in recent molecular dynamics (MD) simulations by Flenner *et al.* [43].

Obviously, at the largest measured q, the normalized polarization $S(q,t)/S(q)$ still does not decay to zero. Thus, the dynamics are not fully covered within the probed window, motivating our choice of an additional longer wavelength to extend the range towards longer Fourier times. At a higher wavelength, a smaller q-range is covered with higher resolution, thus two complementary data sets are obtained by the combination of wavelengths.

4.2.2 Long-wavelength dynamics: Bilayer undulations and vesicle mass diffusion

The local lipid bilayer undulation dynamics was measured on IN15 at a wavelength of $\lambda = 18\,\text{Å}$. The normalized intermediate scattering function of the DMPC standard $S(q,t)/S(q)$ for varying q is shown in fig. 4(a). The covered Fourier times extend up to 285 ns, and the normalized polarization decays to less than 0.1, which lies very close to a full polarization decay, at the largest momentum transfers q. Thus, in this (q,t)-range, the dynamics are better captured within the spectrometer window, enabling more analytic fits. We find that over the whole q-range, these fits can be improved taking into account dynamic contributions just outside the instrumental window in the μs regime. Therefore, we add a vesicle center-of-mass diffusion contribution by injecting the bulk diffusion constant D obtained from dynamic light scattering experiments into the expression given by eq. (2). In fig. 4(b), both vesicle mass diffusion and bilayer undulation contributions are indicated on a double logarithmic scale for the pure DMPC standard for one exemplary

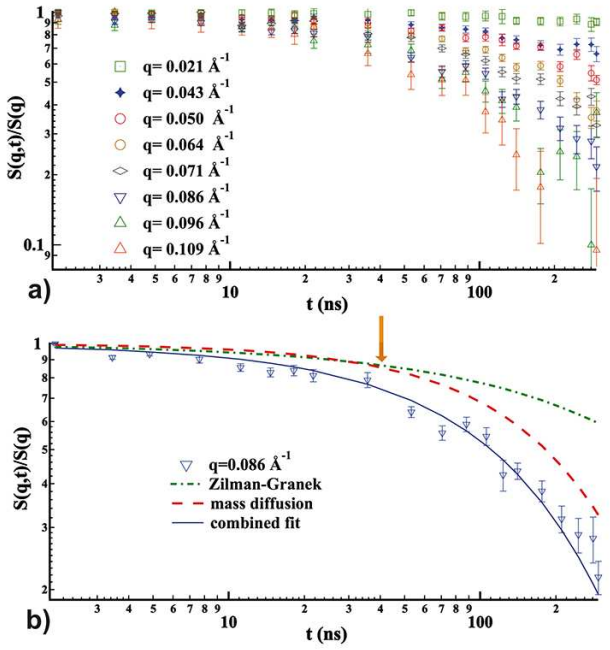

Fig. 4. Normalized intermediate scattering functions $S(q,t)/S(q)$ for DMPC standard at 30 °C: (a) whole q-range covered at $\lambda = 18$ Å; (b) combined fit according to eq. (2), single contributions from vesicle center-of-mass diffusion and bilayer undulations, respectively (not weighted).

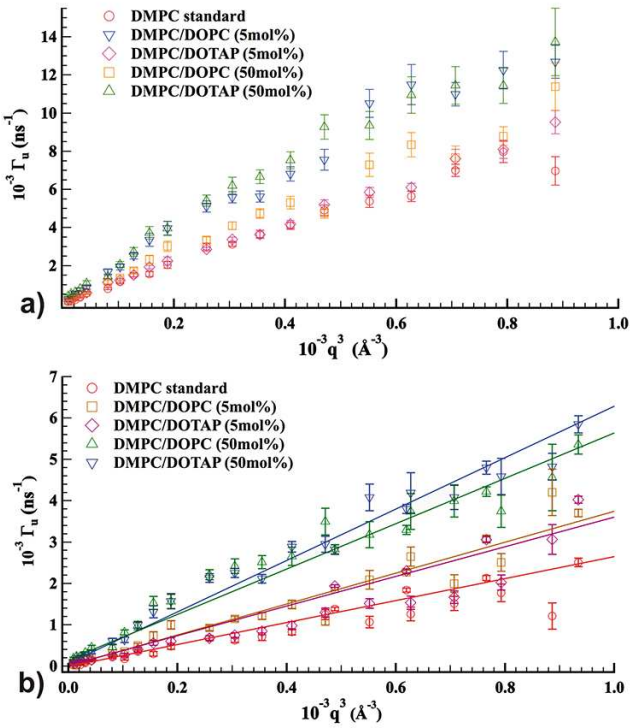

Fig. 5. Undulation relaxation rate $\Gamma_u(q^3)$: (a) Zilman-Granek fit (eq. (1)); (b) combined fit using Zilman-Granek and vesicle mass diffusion contributions (eq. (2)). The difference in the relaxation rate Γ_u obtained from the two types of fits lies roughly on the order of two.

q-value. Here, one can see that up to Fourier times of 40 ns, the two dynamic contributions can hardly be distinguished. At longer Fourier times, on the other hand, the decay curvature exhibits an intermediate behaviour, that is well matched by the combined fit. At momentum transfers of $q = 0.071$ Å and above, this deviation from the single-exponential behaviour is observed to start at Fourier times between 40 and 50 ns. Thus, by applying combined fits (eq. (2)), the undulation relaxation rate $\Gamma_u(q)$ can be more clearly separated and analyzed.

In particular, for the DMPC standard in its fluid phase (30 °C), the result of $\kappa = 17.68 \pm 0.15 k_BT$ derived from linear regression of $\Gamma_u(q^3)$ is well in accordance with literature values [14, 44, 45]. The inherent experimental error for κ is estimated to lie on the order of k_BT. For several exemplary lipid mixtures, the undulation relaxation rate $\Gamma_u(q^3)$ is plotted in fig. 5 for two types of fits, respectively: (a) taking into account merely bilayer undulations described by Zilman and Granek, and (b) both undulations and vesicle center-of-mass diffusion. One can see that the obtained undulation relaxation rates $\Gamma_u(q^3)$ differ by roughly a factor of two. Thus, the influence of vesicle center-of-mass diffusion is significant and has to be taken into account in order to obtain plausible values for the bilayer bending rigidities κ. With these rather unrestrictive assumptions for the data analysis, we yield a $\Gamma_u(q^3)/q^3 \sim \kappa$ for pure DMPC from the combined fit (eq. (2)), that lies very close to the one obtained by Arriaga *et al.* for their single lipid standard [19]: the authors treat their data as an equally weighted sum of two decays, which correspond to vesicle mass diffusion and bilayer undulations, respectively. Further, taking into account that Yi *et al.* find that bilayer bending rigidities of single lipids hardly depend on the respective acyl chain properties [31], these literature results can in effect be quantitatively related to ours. The fits are performed for all lipid mixtures, the bilayer bending rigidities κ derived from the undulation relaxation rate $\Gamma_u(q^3)$ are summarized in table 1.

For the investigated lipid mixtures, two interesting observations could be made: Already small amounts of added unsaturated lipid evoke a distinct decrease in the bilayer bending rigidity κ (softening). With increasing amount of unsaturated lipid, the obtained difference in κ between the mixtures containing the respective cationic and zwitterionic components decreases, until it is hardly distinguishable from the treatment error at equimolar lipid ratio. In fact, a similar observation was made in a previous study, where the effect of charge density on the bending rigidity of the amphiphillic film of microemulsion droplets was investigated [29]. There, the bending elasticity was derived independently using the two methods of neutron small-angle scattering and neutron spin-echo spectroscopy. Contrary to theoretical suggestions [46–50], charges evoked no changes in the rigidity of the model film within experimental resolution. Also in our case, the lipid headgroup charge does not cause the most prominent changes in the bilayer bending rigidity: regarding the bilayer softening at rising concentrations of unsaturated lipid, a similar tendency is

Table 1. Bilayer bending rigidity κ derived from linear fit of the separated undulation relaxation rate $\Gamma_u(q^3)$ (eqs. (1), (2)). The fit error corresponds to $\Delta\kappa/\kappa \approx 0.15$.

	DMPC/DOPC	DMPC/DOTAP
Conc. (mol%)	κ (k_BT)	κ (k_BT)
0	17.7 ± 2.7	17.7 ± 2.7
5	6.5 ± 1.0	5.8 ± 0.9
10	2.9 ± 0.4	3.3 ± 0.5
50	1.8 ± 0.3	1.5 ± 0.2

observed for both charged and uncharged mixtures. Where they exceed the experimental error, observed differences between the two lipid mixtures could be caused either by electrostatic repulsion between charged headgroups on the nearest neighbour scale, or a feature of slightly different domain formation in the lipid bilayer plane with respect to the corresponding reference lipid mixture. Further, an increase in the bilayer asymmetry between the inner and the outer leaflet of the vesicle should increase with rising amounts of charged lipid. The corresponding bilayer and vesicle curvature would change accordingly due to changes in the interfacial tension, thus causing a shift in the bilayer bending rigidity κ with respect to the uncharged reference. Nevertheless, at the equimolar ratio the difference obtained in the bending rigidity κ for the two lipid mixtures only slightly exceeds the experimental error. On the basis of the theoretically predicted electrostatic contribution to the bending elasticity [46–52], one would rather expect a larger κ for the charged liposomes (DMPC/DOTAP). In the future, charge-induced changes in vesicle size and interface line tension could possibly be more readily accessible experimentally through dynamic light scattering experiments on giant unilamellar vesicles (GUVs). Here, the vesicle size exceeds the presently investigated ones by at least an order of magnitude, and instead of local bilayer undulations around an equilibrium position, characteristic averaged shape fluctuations of whole vesicles are probed in the form of second order spherical harmonics.

Our second observation is that, within the lipid mixtures, acyl chain unsaturation in one of the components affects the bilayer bending rigidity much stronger, than the presence of a headgroup charge. While at the low wavelength a maximum in the overall diffusion coefficient D_f was obtained in both cases for 10 mol% of unsaturated lipid, the long-wavelength undulations follow a monotonous trend with changing composition of the lipid mixture: a bilayer softening at rising concentrations of unsaturated lipid is observed for both charged and uncharged lipid mixtures. The coupling of these two modes will be discussed in more detail in a forthcoming contribution [53].

The bilayer softening with increasing heterogenity of the mixture is believed to be a consequence of the mismatch between the hydrophobic acyl chains of the respective lipids, which causes a lateral segregation in the membrane plane (domain formation). Numerous studies have implied that model membranes of two component lipid mixtures form compositionally distinct domains of varying size and distribution across the vesicle, cf. *e.g.* [54–57]. Consequently, several authors have pointed out a link between occurring domain structure fluctuations and the corresponding bilayer bending rigidity κ [26,27]. Changes in the domain structure fluctuations of a DMPC model membrane induced by small quantities of added unsaturated lipid DOPC have been discussed in [25]. Our current results match a picture of a fluidization of the membrane with increasing amount of inserted unsaturated lipid.

5 Conclusion and outlook

We have investigated the effect of lipid head group charge and acyl chain unsaturation on vesicular model membrane mixtures, mainly in view of characteristic local lipid bilayer undulations and bending rigidity κ. In addition, and to place the quasielastic neutron scattering in proper context, effects on vesicle center-of-mass diffusion, size and phase state were also investigated using dynamic light scattering. The neutron spin-echo data can be meaningfully analyzed, assuming a combination of two separable contributions within the dynamic window up to 285 ns, namely vesicle center-of-mass diffusion and local lipid bilayer undulations. The latter contribution was described on the basis of the well-known Zilman-Granek approach for free film fluctuations.

Our findings on cationic liposome bilayer bending rigidities κ could have important implications for their use as gene transfer agents: we have shown, that on the local length scale probed around a membrane equilibrium position, changes in the headgroup composition and charge seem to have less of an impact on a vesicle's bilayer stability than variations in the acyl chain order. Thus, cationic liposomes, which are more suitable as carrier vehicles than their zwitterionic counterparts, do not suffer from increased instabilities through their headgroup charges. Moreover, recent studies have emphasized an important link between acyl chain properties in lipid mixtures and the corresponding gene transfection efficiency [11,12]. Encouraged by these findings, we now plan to follow up the presented study by investigating the effect of RNA-loading on bilayer undulation dynamics and bending rigitity κ. Moreover, in future work changes of κ as a function of temperature will also be studied.

We are grateful to HZB for financial support and the allocation of beam time on IN15, as well as to ILL for technical support.

References

1. R.B. Campbell, S.V. Balasubramanian, R.M. Straubinger, J. Pharm. Sci. **90**, 1091 (2001).
2. L.P. Calvacanti, O. Konovalov, H. Haas, Chem. Phys. Lip. **150**, 58 (2007).
3. J. Wang, D. Mongayt, V.P. Torchilin, J. Drug Targ. **13**, 73 (2005).
4. N.J. Zuidam, Y. Barenholz, Biochim. Biophys. Acta **1368**, 115 (1998).

5. P.C. Ross, S.W. Hui, Gene Therapy **6**, 651 (1999).
6. J.-F. Labbé, F. Cronier, R.C.-Gaudreault, M. Auger, Chem. Phys. Lip. **158**, 91 (2009).
7. N.J. Zuidam, Y. Barenholz, Biochim. Biophys. Acta **1329**, 211 (1997).
8. R.B. Campbell, S.V. Balasubramanian, R.M. Straubinger, Biochim. Biophys. Acta **1512**, 27 (2001).
9. M. Gradzielski, J. Phys.: Condens. Matter **15**, R655 (2003).
10. S. Cinelli, G. Onori, S. Zuzzi, F. Bordi, C. Cametti, S. Sennato, J. Phys. Chem. B **111**, 10032 (2007).
11. R. Koynova, B. Tenchov, Soft Matter **5**, 3187 (2009).
12. R. Koynova, B. Tenchov, L. Wang, R.C. MacDonald, Mol. Pharm. **6**, 951 (2009).
13. I. Sikharulidze, B. Farago, I.P. Dolbnya, A. Madsen, W.H. de Jeu, Phys. Rev. Lett. **91**, 165504 (2003).
14. M.C. Rheinstädter, W. Häußler, T. Salditt, Phys. Rev. Lett. **97**, 048103 (2006).
15. J.S. Hub, T. Salditt, M.C. Rheinstädter, B.L. de Groot, Biophys. J. **93**, 3156 (2007).
16. M.C. Rheinstädter, J. Das, E.J. Flenner, B. Brüning, T. Seydel, I. Kosztin, Phys. Rev. Lett. **101**, 248106 (2008).
17. S. Busch, C. Smuda, L.C. Pardo, T. Unruh, J. Am. Chem. Soc. **132**, 3232 (2010).
18. A.C. Woodka, P.D. Butler, L. Porcar, B. Farago, M. Nagao, Phys. Rev. Lett. **109**, 058102 (2012).
19. L.R. Arriaga, I. Lopez-Montero, F. Monroy, G. Orts-Gil, B. Farago, T. Hellweg, Biophys. J. **96**, 3629 (2009).
20. E.G. Brandt, O. Edholm, J. Chem. Phys. **133**, 115101 (2010).
21. E. Flenner, J. Das, M.C. Rheinstädter, I. Kosztin, Phys. Rev. E **79**, 011907 (2009).
22. R. Rodriguez-Garcia, L.R. Arriaga, M. Mell, L.H. Moleiro, I. Lopez-Montero, Phys. Rev. Lett. **102**, 128101 (2009).
23. L.R. Arriaga, R. Rodriguez-Garcia, I. Lopez-Montero, B. Farago, T. Hellweg, F. Monroy, Eur. Phys. J. E **31**, 105 (2010).
24. L.R. Arriaga, I. Lopez-Montero, G. Orts-Gil, B. Farago, T. Hellweg, F. Monroy, Phys. Rev. E **80**, 031908 (2009).
25. B. Brüning, E. Wald, W. Schrader, R. Behrends, U. Kaatze, Soft Matter **5**, 3340 (2009).
26. T. Heimburg, *Thermal Biophysics of Membranes* (Wiley-VHC, Weinheim, Germany, 2007).
27. J.F. Nagle, H.L. Scott Jr., Biochim. Biophys. Acta **513**, 236 (1978).
28. R. Schomäcker, R. Strey, J. Phys. Chem. **98**, 3908 (1994).
29. B. Farago, M. Gradzielski, J. Chem. Phys. **114**, 10105 (2001).
30. Y. Hattori, H. Ushiki, L. Courbin, P. Panizza, Phys. Rev. E **75**, 021504 (2007).
31. Z. Yi, M. Nagao, D.P. Bossev, J. Phys.: Condens. Matter **21**, 155104 (2009).
32. M.B. Boggara, A. Faraone, R. Krishnamoorti, J. Phys. Chem. B **114**, 8061 (2010).
33. J.-H. Lee, S.-M. Choi, C. Doe, A. Faraone, P.A. Pincus, S.R. Kline, Phys. Rev. Lett. **105**, 038101 (2010).
34. W. Helfrich, Z. Naturforsch. C **28**, 693 (1973).
35. S.T. Milner, S.A. Safran, Phys. Rev. A **36**, 4371 (1987).
36. A.G. Zilman, R. Granek, Phys. Rev. Lett. **77**, 4788 (1996).
37. A.G. Zilman, R. Granek, Chem. Phys. **284**, 195 (2002).
38. F. Mezei, *Neutron Spin Echo* (Springer, Berlin, 1980).
39. N.L. Gershfeld, J. Phys. Chem. **93**, 5256 (1989).
40. E. Evans, A. Yeung, Chem. Phys. Lipids **73**, 39 (1994).
41. U. Seifert, S.A. Langer, Europhys. Lett. **23**, 71 (1993).
42. W. Pfeiffer, Th. Henkel, E. Sackmann, W. Knoll, D. Richter, Europhys. Lett. **8**, 201 (1989).
43. E. Flenner, J. Das, M.C. Rheinstädter, I. Kosztin, Phys. Rev. E **79**, 011907 (2009).
44. K.R. Mecke, T. Charitat, F. Graner, Langmuir **19**, 2080 (2003).
45. C.R. Safinya, E.B. Sirota, D. Roux, G.S. Smith, Phys. Rev. Lett. **62**, 1134 (1989).
46. A. Fogden, D.J. Mitchell, B.W. Ninham, Langmuir **6**, 159 (1990).
47. M. Winterhalter, W. Helfrich, J. Phys. Chem. **92**, 6865 (1988).
48. D.J. Mitchell, B.W. Ninham, Langmuir **5**, 1121 (1989).
49. H.N.W. Lekkerkerker, Physica A **159**, 319 (1989).
50. J. Daicic, A. Fogden, I. Carlsson, H. Wennerström, B. Jönsson, Phys. Rev. E **54**, 3984 (1996).
51. S. May, J. Phys. Chem. **105**, 8314 (1996).
52. I. Carlsson, A. Fogden, H. Wennerström, Langmuir **15**, 6150 (1999).
53. B. Brüning, S. Prevost, R. Stehle, R. Steitz, P. Falus, B. Farago, T. Hellweg, submitted.
54. O.G. Mouritsen, Chem. Phys. Lipids **57**, 179 (1991).
55. O.G. Mouritsen, K. Jørgensen, Chem. Phys. Lipids **73**, 3 (1994).
56. L.A. Bagatolli, J.H. Ipsen, A.C. Simonsen, O.G. Mouritsen, Progr. Lipid Res. **49**, 378 (2010).
57. J. Brewer, J. Bernardino de la Serna, K. Wagner, L.A. Bagatolli, Biochim. Biophys. Acta **1798**, 1301 (2010).